3D inversion of the towed streamer EM data using the seismic constraints

Michael S. Zhdanov, TechnoImaging and the University of Utah; Masashi Endo, and David Sunwall, TechnoImaging; Martin Čuma, TechnoImaging and the University of Utah, Jenny-Ann Malmberg, Allan McKay, Tashi Tshering, and Jonathan Midgley, PGS Geophysical AS*

Summary

In this paper we introduce a large-scale 3D inversion technique for towed streamer electromagnetic (EM) data, which incorporates seismic constraints. The inversion algorithm is based on the integral equation (IE) forward modeling and utilizes a re-weighted regularized conjugate gradient method with adaptive regularization to minimize the objective functional. We have also incorporated in the inversion the moving sensitivity domain approach in order to invert the entire large-scale towed streamer EM survey data while keeping the accuracy and reducing the time and memory/storage of the computation. The developed algorithm and software can take into account the constraints based on seismic and well-log data, and provide the inversion guided by these constraints. Application of the developed method to the interpretation of the large-scale towed streamer EM survey data acquired in the Barents Sea demonstrates its practical effectiveness.

Introduction

Development of the towed streamer EM system by PGS made it possible to acquire EM data over very large areas rapidly and with high accuracy. In the papers by Zhdanov et al. (2014a, b) an effective method for 3D inversion of the towed streamer EM data based on the contraction integral equation method and the concept of the moving sensitivity domain (Zhdanov and Cox, 2013) was developed. The regularized inversion was implemented using the re-weighted regularized conjugate gradient (RRCG) method with adaptive regularization to minimize the objective functional (Zhdanov, 2015).

It is well known that the seismic method has higher resolution to the interfaces between different geological formations, than the EM method, while the latter has higher sensitivity to the presence of hydrocarbons (HC) in the reservoir rocks. In order to combine the advantages of both geophysical techniques, it is important for EM inversion to take into account seismic information about the geological boundaries. However, it is not necessary to impose strict constraints with fixed positions of the boundaries, which may not adequately represent the geoelectrical model. We have developed a method of "guided" inversion, which imposes soft constraints, allowing for the boundaries to be updated during the inversion process. In other words, the seismically guided inversion is still driven by the EM data, but it takes into account the known seismic horizons.

We have applied the developed seismically guided EM inversion to data collected in a large-scale (approximately 2000 line kms) towed streamer EM survey, conducted in the Barents Sea in 2014.

Inversion methodology and workflow

3D inversion of towed streamer EM data is a very challenging problem because of the huge number of transmitter positions of the moving towed streamer EM system, and, correspondingly, the huge number of 3D forward and inverse problems that need to be solved for every transmitter position over the large survey area. We overcame this problem by using the moving sensitivity domain approach (Zhdanov et al., 2014a, b).

There are several important components/steps of the developed inversion method:

1) 1D inversions of the towed streamer EM data - determination of a general (variable) background geoelectrical model
2) 3D unconstrained inversion of the towed streamer EM data:
    - Construction of the a priori model (variable background) based on 1D inversion results and known information, such as bathymetry and seawater conductivity
    - 3D unconstrained inversion with variable background
3) 3D constrained/guided inversion of the towed streamer EM data:
    - Construction of the a priori model based on 3D unconstrained inversion results and seismic data (seismic horizons)
    - 3D constrained/guided inversion with the constructed a priori model

Note that, even in the case of 3D constrained/guided inversion, all resistivity values in the inversion domain are still free to change to minimize the parametric functional. In other words, the a priori model only guides the solution towards a more geologically plausible model, while maintaining a similar level of the misfit between the observed and predicted data (Zhdanov et al., 2014 a, b). Figure 1 summarizes the workflow above.

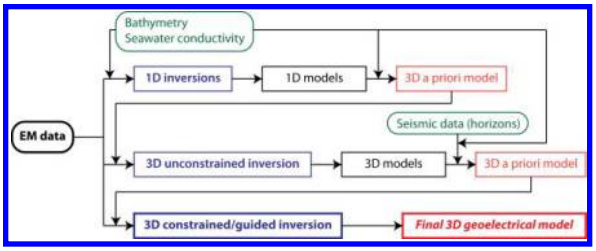

Figure 1: A workflow of the 3D constrained/guided inversion.

Towed streamer EM survey in the Barents Sea

The Barents Sea was formed by two major continental collisions and subsequent separation. The first event was the Caledonian orogeny, some 400 Ma. The Caledonian fold belt runs N-S through Scandinavia and the Svalbard Archipelago and mainly influences the western part of the Barents Sea. The second collision event was the Uralian orogeny, about 240 Ma. Running from East Russia up along Novaya Zemlya, the Uralian fold belt has caused an N-S structural grain in the rocks of the eastern Barents Sea (Doré, 1994).

The most significant proportion of the HC reserves proven to date in both the Norwegian and Russian Barents Sea is contained within the strata of Jurassic age. The major discoveries in the Norwegian sector, e.g., Snøhvit, all have the principal reservoir consisting of Lower – Middle Jurassic sandstone. This unit was deposited in a coastal marine setting and, where penetrated in the Hammerfest Basin, usually had very favorable reservoir properties (high porosity and permeability). Larsen et al. (1993) have estimated that about 85 % of the Norwegian Barents Sea HC resources lay within this formation. The traps that form the Norwegian Jurassic fields are generally fault-bounded positive blocks, and the HC are sealed by overlaying Upper Jurassic shales (Doré, 1994).

More than 10000 line-km of EM data were acquired in the Barents Sea in 2014 by the current generation of the towed streamer EM system. The towed streamer EM survey was conducted using an 800 m long bi-pole electric current source with 1500 Amperes current towed at a depth of 10 m, and the streamer cable which measured in-line electric fields with offsets from 0 to 7733 m in a frequency range from 0.2 to 9.8 Hz at a depth of 100 m from the sea surface. In the current inversion study, we used a total of 2167 line-km of the towed streamer EM data covering the survey area of ~ 1500 sq. km (Figure 2) with offsets from 1888 to 7733 m in a frequency range from 0.2 to 3.0 Hz.

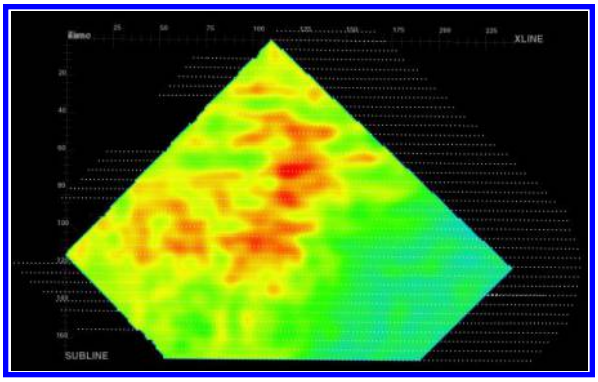

Figure 2: A shot point map of the towed streamer EM survey in the Barents Sea and a depth slice at ~700 m of the horizontal resistivity recovered from the guided inversion. The shot interval is 250 m and the line spacing is 1.25 km.

Inversion results

The inversion domain consisted of 63 M cells, and was 84 km in the x direction (parallel to the survey lines), 44 km in the y direction (perpendicular to the survey lines), and 3 km in the z direction. The cells were 50 m x 50 m in horizontal directions, and from 12.5 m to 200 m (total 43 layers) in the vertical direction. The selected towed streamer EM data for the inversion consisted of a total 594,125 data points with 24 offsets (approximately from 1,900 m to 7,700 m) and seven frequencies (from 0.2 Hz to 3.0 Hz) along 37 survey lines (Figure 2).

Figure 3 shows an example of the vertical cross section of 3D anisotropic geoelectrical model recovered from 3D unconstrained inversion overlain with 3D seismic data. One can clearly see a thin resistive layer in the shallow region, at a depth consistent with Jurassic sediments. For a comparison, Figure 4 shows a vertical cross section of the geoelectrical model recovered from 2.5D inversion along the same survey line. The 2.5D inversion results were obtained using a parallel adaptive finite element code for inverse modeling of marine electromagnetic geophysics (Key et al., 2014). The main features recovered from the two different inversion schemes are similar, indicating that the recovered geoelectrical structures represent the sea-bottom geological formations correctly.

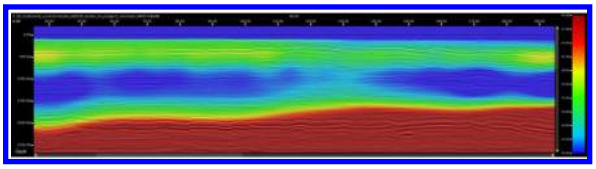

Figure 3: Vertical cross section of the 3D vertical resistivity (20-50Ωm) recovered from 3D unconstrained inversion along a survey line overlain with 3D seismic data.

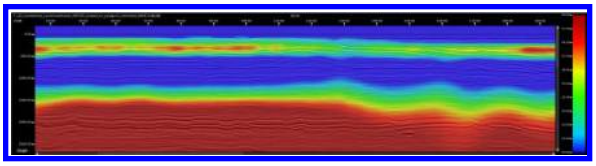

Figure 4: Vertical cross section of the vertical resistivity (20-50Ωm) recovered from 2.5D unconstrained inversion along a survey line overlain with 3D seismic data.

Figure 5 shows vertical cross sections of 3D a priori model; (a) vertical resistivity, and (b) horizontal resistivity, constructed from the 3D model recovered from 3D unconstrained inversion and surfaces interpreted from seismic data. The following surfaces were used to construct a 3D a priori model:

– Seafloor (bathymetry)
– Base Cretaceous
– Near Top Jurassic
– Top Triassic
– Mid-Triassic

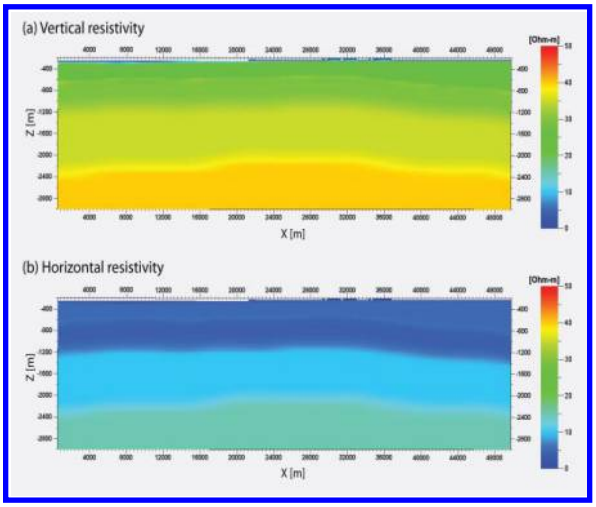

Figure 5: Vertical cross sections, (a) vertical resistivity and (b) horizontal resistivity, of 3D a priori model used for the 3D seismically guided inversion.

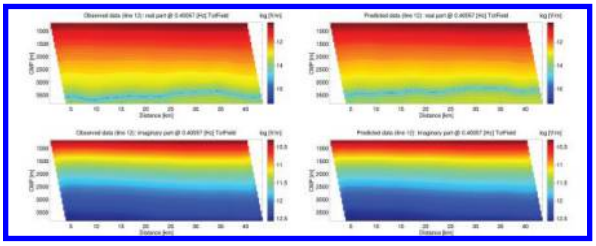

Figure 6: CMP plots of the observed (left panels) and predicted (right panels) towed streamer EM data at a frequency of 0.4 Hz. The top panels show the real part of the data while the bottom panels show the imaginary part of the data.

Figure 6 shows examples of CMP plots of the observed (left panels) and predicted (right panels) towed streamer EM data. In this figure, top panels show the real part while bottom panels show the imaginary part of the data. One can see that the predicted data agree very well with the observed data, and the normalized misfit (the L2 norm of the residual between predicted and observed data, normalized by the L2 norm of the observed data) converged into 2.4 %.

Figures 7, 8 and 9 show an example of the vertical and horizontal cross sections of the 3D anisotropic geoelectrical model, vertical resistivity, horizontal resistivity, and anisotropic coefficient (the ratio of the vertical resistivity over the horizontal resistivity), recovered from 3D seismically guided inversion. One can clearly see that the recovered geoelectrical model is improved in comparison with the model recovered from the unconstrained inversion, with a crisper imaging of the shallow features and improved definition of deeper resistive anomalies. The shallower resistive layer indicates potentially interesting resistive features in the Jurassic formation, while the model shows regions of anomalously high resistivity deeper in the Triassic. Especially for the case of the anisotropic coefficient (Figure 9), the formation can be estimated more clearly.

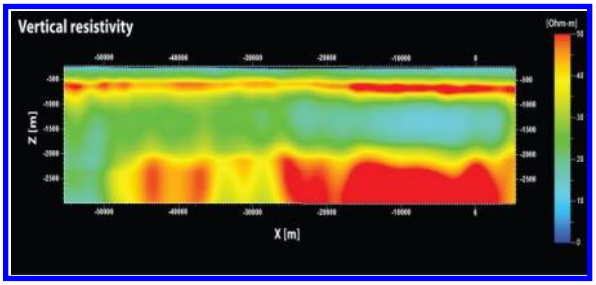

Figure 7: An example of the vertical cross-section of the 3D vertical resistivity distribution recovered from 3D seismically guided inversion.

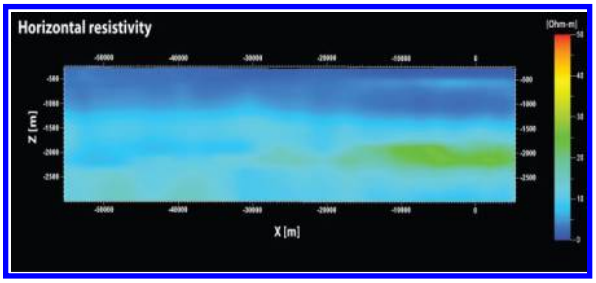

Figure 8: An example of the vertical cross section of the 3D horizontal resistivity distribution recovered from 3D seismically guided inversion.

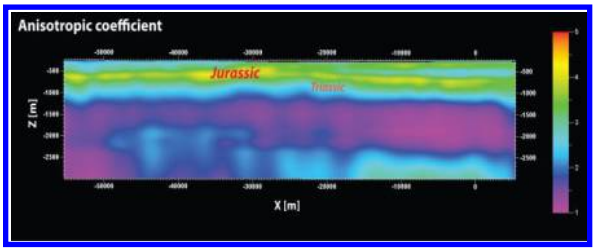

Figure 9: An example of the 3D anisotropic coefficient (ratio of the vertical resistivity over the horizontal resistivity) distribution recovered from 3D seismically guided inversion.

Figure 10, 11, and 12 show 3D views of the 3D vertical resistivity distribution, 3D horizontal resistivity distribution, and 3D anisotropic coefficient distribution, recovered from 3D seismically guided inversion. In these figures, the top level of the 3D volumes is 700 m below the sea surface.

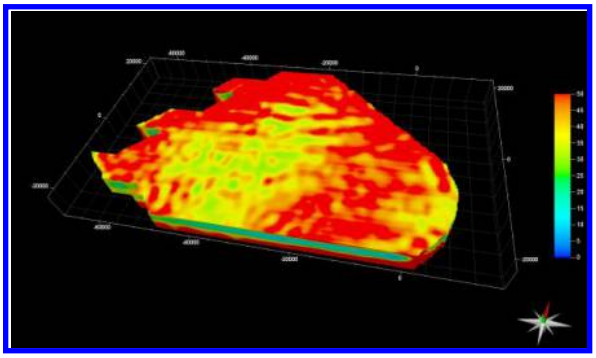

Figure 10: A 3D view of the 3D vertical resistivity distribution recovered from 3D seismically guided inversion. The top level of the 3D volume is 700 m below the sea surface.

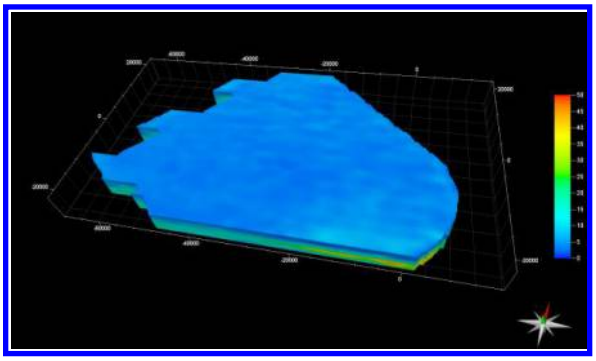

Figure 11: A 3D view of the 3D horizontal resistivity distribution recovered from 3D seismically guided inversion. The top level of the 3D volume is 700 m below the sea surface.

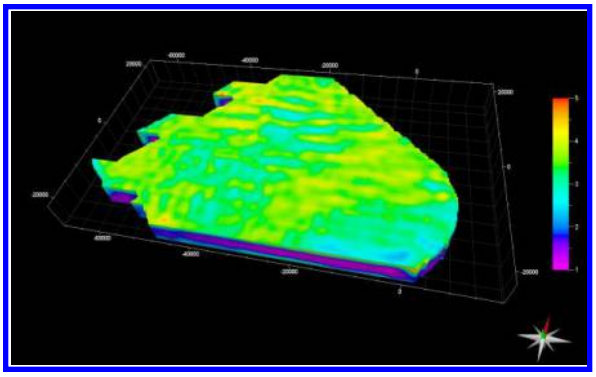

Figure 12: A 3D view of the 3D anisotropic coefficient distribution recovered from 3D seismically guided inversion. The top level of the 3D volume is 700 m below the sea surface.

Conclusions

We have developed an approach to incorporate seismic constraints in the 3D EM inversion algorithm, based on the 3D contraction integral equation method and the concept of a moving sensitivity domain. The seismically guided anisotropic inversion of the large-scale towed streamer EM survey, acquired over the Barents Sea, produced a resistivity anomaly that agreed well with the general geological structures in the survey area and other available geophysical information. The new method of seismically guided EM inversion has proven to be efficient for a large towed streamer EM dataset in a complex geological setting.

Acknowledgements

The authors thank PGS and TechnoImaging for support of this research and permission to publish.

EDITED REFERENCES

Note: This reference list is a copyedited version of the reference list submitted by the author. Reference lists for the 2016 SEG Technical Program Expanded Abstracts have been copyedited so that references provided with the online metadata for each paper will achieve a high degree of linking to cited sources that appear on the Web.

REFERENCES

Dore, A. G., 1994, Barents geology, petroleum resources and commercial potential: Arctic Institute of North America, **48**, 207–221.

Key, K., Z. Du, J. Mattsson, A. McKay, and J. Midgley, 2014, Anisotropic 2.5D inversion of Towed Streamer EM data from three North Sea fields using parallel adaptive finite elements: 76th Annual International Conference and Exhibition, EAGE, Extended Abstracts, http://dx.doi.org/10.3997/2214-4609.20140730.

Larsen, R. M., T. Fjæran, and O. Skarpnes, 1993, Hydrocarbon potential of the Norwegian Barents Sea based on recent well results, *in* T. O. Vorren, E. Bergsager, Ø. A. Dahl-Stamnes, E. Holter, B. Johansen, E. Lie, and T. B. Lund, eds., Arctic geology and petroleum potential: NPF Special Publication, **2**, 321–331, http://dx.doi.org/10.1016/B978-0-444-88943-0.50025-3.

Zhdanov, M. S., 2015, Inverse theory and applications in geophysics: Elsevier.

Zhdanov, M. S., and L. H. Cox, 2012, Method of real time subsurface imaging using electromagnetic data acquired from moving platform: U.S. Patent US 13/488,256.

Zhdanov, M. S., M. Endo, L. H. Cox, M. Cuma, J. Linfoot, C. Anderson, N. Black, and A. V. Gribenko, 2014a, Three-dimensional inversion of towed streamer electromagnetic data: Geophysical Prospecting, **62**, 552–572, http://dx.doi.org/10.1111/1365-2478.12097.

Zhdanov, M. S., M. Endo, D. Sunwall, and J. Mattsson, 2015, Advanced 3D imaging of complex geoelectrical structures using towed streamer EM data over the Mariner field in the North Sea: First Break, **33**, 59–63.

Zhdanov, M. S., M. Endo, D. Yoon, M. Čuma, J. Mattsson, and J. Midgley, 2014b, Anisotropic 3D inversion of towed-streamer electromagnetic data: Case study from the Troll West Oil Province: Interpretation, **2**, SH97–SH113, http://dx.doi.org/10.1190/INT-2013-0156.1.